Thermochimica Acta, 189 (1991) 313–350
Elsevier Science Publishers B.V., Amsterdam

Review

A review of the application of thermal analysis to cement–admixture systems

Javed I. Bhatty

Mineral Resources Research Center, 56 East River Road, University of Minnesota, Minneapolis, MN 55455 (USA)

(Received 27 February 1991)

Abstract

The application of thermal analysis in the investigation of the role of chemical admixtures in cement hydration is reviewed. The relevant literature published on DTA, TG and DTG techniques during the past two decades has covered both the kinetic and mechanism aspects of cement hydration, with or without the presence of accelerators, retarders/water reducers and plasticizers. Two vital components of cement, namely C_3S and C_3A, have been of particular interest to researchers, C_3S being the major compound controlling the overall hydration, and C_3A being the most reactive component controlling the initial setting of the cement. Modifications of various products that develop in cement pastes in the presence of admixtures as monitored by thermal analysis are quoted frequently in this review in order to elucidate the mechanism of the action of admixtures on the cement hydration.

INTRODUCTION

During the last two decades, the use of thermal analysis in the cement industry has found diverse applications and has led to a better understanding and appreciation of numerous practical situations. The ability of thermal analysis to detect minor chemical changes and to provide analytical information on individual cement phases and hydration products makes it one of the foremost analytical techniques, along with X-ray diffraction and scanning electron microscopy. Reviews by Ramachandran [1], Barta [2], MacKenzie [3] and, more recently, by Ben-Dor [4] have covered the application, techniques and interpretations of thermal analysis in cement sciences. The technique is convenient, fast and accurate, and provides additional information which is not readily available using other techniques.

Numerous workers have contributed towards the application of thermal analysis to the study of the hydration characteristics of cement, with or without the presence of chemical admixtures such as accelerators, retarders, water reducers, plasticizers and air-entraining agents. A distinction must be made between chemical admixtures which react chemically with the cement and are added in quantities less than 1% by weight of cement and other materials such as fly ash and ground, granulated blast-furnace slags which

0040-6031/91/$03.50

have cementitious properties and are added as cement replacements in amounts up to 90 : 10 admixture–cement. This review deals only with studies of chemical admixtures in terms of their mode of action, as revealed by the application of thermoanalytical techniques. The work of Ramachandran, Ben-Dor, Bensted, El-Jazairi, Illston, Midgley, Maycock, Jawed, Skalny, Singh, and Dollimore, together with Bhatty, and Mitsuda, Taylor, and Dent-Glasser and co-workers [5–45] has been frequently referred to this context. Ramachandran and co-workers [5–12] studied the hydration of cement and individual phases in the presence of accelerators, retarders and superplasticizers; Ben-Dor and co-workers [13–16] and Bensted [17–21] studied the effect of accelerators; Singh [22,23], Dollimore, Bhatty and co-workers [24–31], Mitsuda, Taylor and Dent-Glasser and co-workers [32–35] studied the formation of calcium silicate hydrate and calcium hydroxide during the hydration of cement pastes, with or without the presence of retarders and other polymer-based admixtures, Skalny, Jawed, and Maycock and co-workers [36–39] applied thermal analysis techniques to the study of individual hydrating phases; El-Jazairi and Illston [40–43] devised a semi-isothermal approach to the study of cement hydration; Midgley and Rosaman [44,45] proposed a method for estimating free calcium hydroxide in hydrated cement.

Calcium hydroxide is a vital component that comprises over 20% of the hydration products in a fully cured cement paste. Estimation of the calcium hydroxide content determines both the hydration characteristics and the degree of hydration of a given cement paste.

CHEMICAL ADMIXTURES

Most of the cement-based concretes produced these days contain one or more admixtures. According to the ASTM definition, an admixture is any material other than water, aggregate or cement used as an ingredient of concrete or mortar and added to the batch immediately before or during mixing. Admixtures are generally classified as accelerators, water-reducers (including retarders, plasticizers and superplasticizers) and air-entraining agents. They impart numerous beneficial effects such as early strength development, accelerated or delayed setting times, improved workability without increasing the water requirement, and better chemical resistance. An account of the global consumption of admixtures during the years 1971–1981 is presented in Table 1 [46]. Although a variety of admixtures are available commercially, it is possible to categorize them according to their basic chemical structures [46,47].

Accelerators

The formulations of accelerators are based on two major raw materials: calcium chlorides and calcium formates with minor amounts of other

TABLE 1

World production and consumption of admixtures and Portland cement 1971–1981 [46]

Geographical area	Estimated cement consumption (million tons)		Estimated [a] admixture consumption (thousand tons)	
	1971	1981	1971	1981
USA	70	70	200	250
South America	40	60	40	40
Western Europe	155	160	100	220
Africa	25	40	10	15
Middle East	N/A	35	10	50
Far East	105	140	80	165
Australia	5	6	5	15

[a] Excluding calcium chloride accelerators.

material such as calcium nitrate, thiosulphate, carbonates and triethanolamine (TEA) which are occasionally included in the formulation.

Water reducers / retarders

Water reducers have a set retarding ability, and can also come under the category of retarders. Most water reducers are derived from wood resins, petroleum by-products or hydroxylated polymers and sugars. The admixtures obtained from formaldehyde derivatives have high molecular weights; they impart greater water-reducing effects and are known as superplasticizers. The most commonly used water reducers/retarders are: lignosulfonates, sugars, hydroxycarboxylic acids and their salts, and formaldehydes.

Air entrainers

Air entrainers are derived from different chemical surfactants; they include (in decreasing order of use in industry): salts of abietic and pimeric acids, salts of fatty acids, alkyl-aryl sulfonates and sulfates and phenol ethoxylates.

A summary of chemical admixtures and their ability to impart specific effects on cement–water systems is given in Table 2.

DTA techniques have been extensively used in studying the role of admixtures in hydrating Portland cement and its components, particularly tricalcium silicate and tricalcium aluminate, respectively the major and most reactive components, controlling the overall hydration kinetics of water–cement systems. Parallel studies by conduction calorimetry and X-ray diffraction are also frequently made to supplement the DTA findings. The hydration behavior of different components are also gauged by their heat evolution characteristics recorded via isothermal conduction calorimetry. Typical

TABLE 2

Summary of types, chemistry and typical effects of chemical admixtures used in the cement and concrete industry

Admixtures	Chemistry	Typical effects	Remarks
Accelerators	Calcium chloride Calcium formates Sodium nitrite	Rapid setting and strength development	Potential risk of corrosion to the reinforcing steel
Retarders	Hydroxycarboxylic acids	Delay setting	May increase bleeding
Water reducers	Lignosulfonate (calcium and sodium salts)	Promote workability at low water consumptions	Potential risk of segregation
Superplasticizers	Sulfonated melamine- and naphthalene-formaldehyde	Facilitate workability over wider range	May increase the risk of segregation
Air-entraining agents	Fatty acids Wood resins	Induce small air bubbles in concrete, increase frost resistance	Workability may increase unnecessarily
Antifreezing agents	Sodium chloride Sodium nitrite Nitrite phase Nitrate + urea	Lower freezing point of the liquid phase of concrete	Extra safety precautions, fire hazards

plots and data on heats of hydration for individual components are given in Fig. 1 and Table 3 respectively. The effect of the admixtures is to extend or reduce the length of the induction period, referred to as the length between the first and second peaks in Fig. 1. Accelerators decrease this period by promoting the hydration process; whereas retarders extend it by inhibiting the hydration process. Wilding et al. [48] employed conduction calorimetry in the classification of chemical admixtures by correlating the time and the rate of maximum heat evolution for cement pastes containing different admixtures. Classification for both retarders and accelerators is shown in Fig. 2.

In DTA and TGA techniques, hydration is usually measured in terms of an estimation of the calcium hydroxide and chemically bound water contents, which reflect the formation, composition and modification of the major hydration products such as calcium silicate hydrate, calcium aluminate hydrate, hexagonal and cubic hydrates, ettringite, monosulfates and other complexes that may form in a given hydrating cement paste.

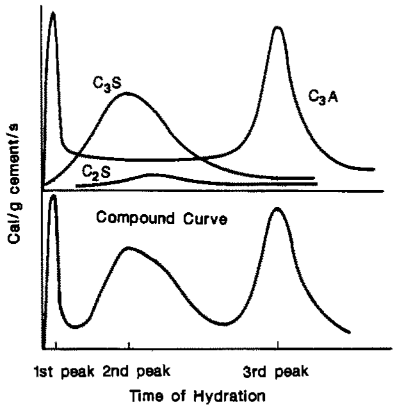

Fig. 1. Typical compound conduction calorimetric curve of cement showing contributions of C_3S, C_2S and C_3A phases.

TABLE 3

Heats of hydration of different cement compounds

Compounds	$J\ g^{-1}$
C_3S	500
C_2S	250
C_3A	1340
C_4AF	420
Portland cements	375–525

As the effects of admixtures depend largely on the hydration characteristics of the individual cement components, a brief description of the hydration of each pure phase, i.e. without the presence of admixtures, would be useful here.

Tricalcium silicate (C_3S) and dicalcium silicate (C_2S) [a]

Both C_3S and C_2S react with water to form calcium silicate hydrate (C–S–H) and calcium hydroxide (CH) as their principal hydration products according to the equations

$$2C_3S + 6H \rightarrow C_3S_2H_3 + 3CH \qquad (1)$$

$$2C_2S + 4H \rightarrow C_3S_2H_3 + CH \qquad (2)$$

The product $C_3S_2H_3$ is commonly referred to as calcium silicate hydrate or

---

[a] Cement chemist notations: $C = CaO$; $S = SiO_2$; $A = Al_2O_3$; $F = Fe_2O_3$; $H = H_2O$; $\bar{S} = SO_3$.

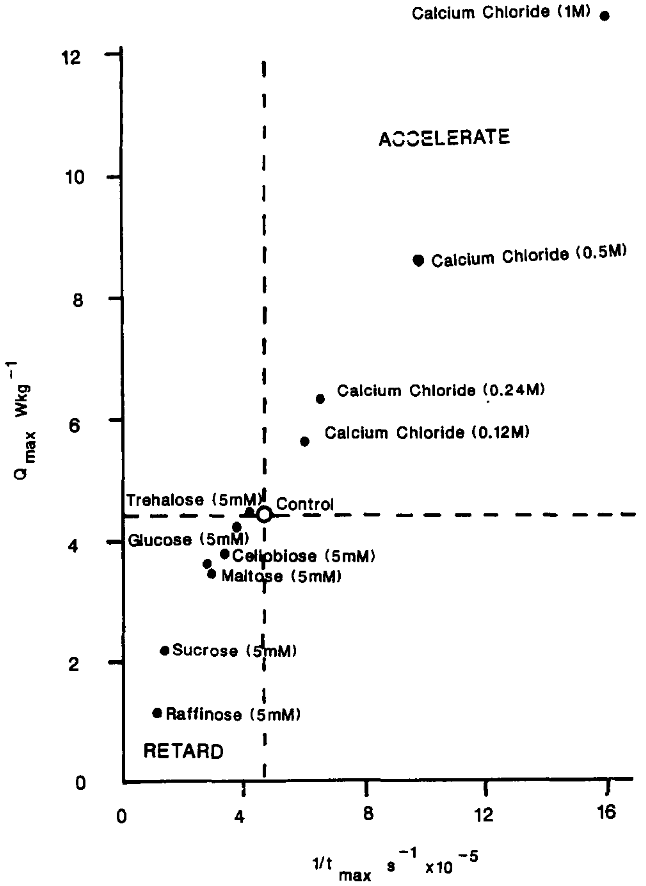

Fig. 2. Classification of chemical admixtures using isothermal conduction calorimetry data [48].

C–S–H gel. The formula $Ca_3SiO_2O_7.3H_2O$ is only a rough approximation as the product is non-stoichiometric and more than one form of this hydrate is possible.

The thermograms of hydrated C_3S and C_2S show similarities, though C_2S has not been studied extensively [18]; early DTA studies on C_2S include those by Midgley [49], Tamas [50], Petzold and Gohlert [51] and Mikhail et al. [52].

In both C_3S and C_2S pastes, endotherms occur around 180 °C showing dehydration reactions due to the loss of water from C–S–H; between 440 and 580 °C, well defined endotherms occur due to the dehydroxylation of the CH formed during hydration; between 780 and 1000 °C, decarbonation of calcium carbonate occurs, together with possible solid–solid phase transitions. Typical thermograms of hydrated C_2S and C_3S are shown in Fig. 3. The dotted lines represent the weight losses. The rate of hydration of C_2S is much slower than that of C_3S, as can be seen from the DTA and TGA plots

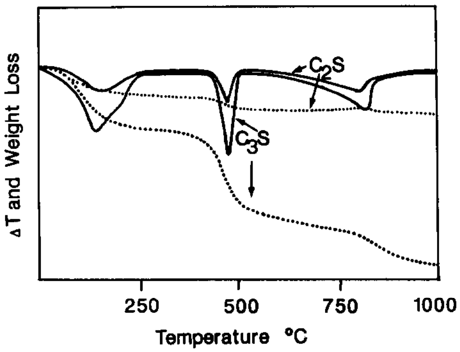

Fig. 3. Typical DTA plot of hydrated cement paste; accompanying weight losses are shown by the TGA plot (dotted lines).

in Fig. 3. Tamas [50] estimated that at 200 days hydration, the weight loss for C_2S is 4%, compared to 13% for C_3S at 21 days.

Hydration products contain bound water incorporated within the C–S–H gel and free CH that precipitates from the lime-rich aqueous phase. El-Jazairi and Illston [42,43] calculated the amount of bound water and free CH from the weight losses during the dehydration, dehydroxylation and decarbonation periods.

Midgley and Rosaman [44,45], Ramachandran [5], Dollimore and co-workers [24,25], and Bhatty and co-workers [26–29] used DTA for estimating the CH content by constructing calibration plots from the endothermic peak areas obtained in the temperature range 410–560 °C for mixtures of alumina and CH or C_3S. The endothermic peak is caused by the decomposition of CH to lime (CaO) and H_2O. A good linear relationship for samples containing up to 20% CH verifies the applicability of the DTA technique [53]. A calibration plot of CH against peak area is given in Fig. 4.

Tricalcium aluminate (C_3A)

At ambient temperature, C_3A hydrates rapidly to form the hexagonal hydrates C_2AH_8 and C_4AH_{13}, which convert to stable cubic hydrate C_3AH_6 with time or if the temperature is sufficiently high ($> 40\,^\circ C$). The reactions takes place as follows

$$2C_3A + 21H \xrightarrow{\text{room temp.}} C_2AH_8 + C_4AH_{13} \text{ (hexagonal hydrates)} \tag{3}$$

$$\xrightarrow{> 40\,^\circ C} 2C_3AH_6 \text{ (cubic hydrate)} + 9H \tag{4}$$

The use of thermal analysis in the study of C_3A hydration has been applied by numerous workers including Midgley and Rosaman [44], Ramachandran and Feldman [7,9,10], Stava and Veprek [54–56], Singh [22], Chebotnikov and Shalinets [57], and Lorprayoon and Rossington [58].

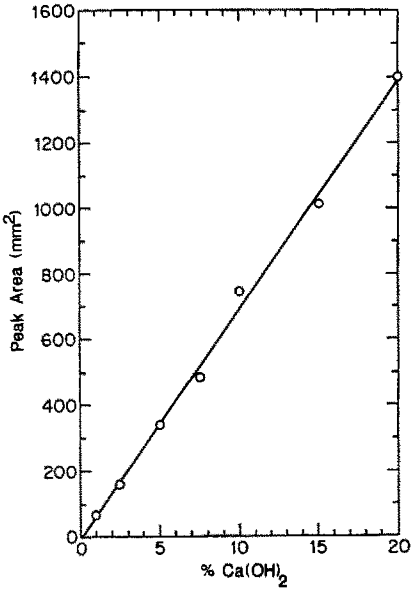

Fig. 4. Calibration curve between calcium hydroxide content and peak area for a hydrated cement paste [26].

The most common DTA thermograms of hydrated C_3A at room temperature are shown in Fig. 5. In the early stages of hydration, up to 2 hours, endothermic peaks at 170 and 245 °C indicate the formation of hexagonal hydrates. Above this, the intense endothermic peaks at 310 and 490 °C indicate the presence of cubic C_3AH_6 phase. These peaks become significantly larger with time, suggesting a gradual conversion of the hexagonal hydrates to the cubic hydrate C_3AH_6. Another distinct endothermic bulge which normally occurs at 315–330 °C is due to C_3AH_6.

Hydration of C_3A in the presence of gypsum

In the presence of gypsum, which is added to avoid flash setting, C_3A undergoes a rapid reaction to form C_4AH_{13} which immediately reacts with calcium sulfate to form ettringite, $C_3A \cdot 3C\bar{S} \cdot H_{32}$. The reactions are

$$C_3A + CH + 12H \rightarrow C_4AH_{13} \text{ (calcium aluminate hydrate)} \quad (5)$$

$$C_4AH_{13} + 3C\bar{S}H_2 + 14H \rightarrow C_3A \cdot 3C\bar{S} \cdot H_{32} \text{ (ettringite)} + CH \quad (6)$$

Ettringite is deposited on the surface of hydrating C_3A and provides an effective barrier to further rapid setting. After all the gypsum has been used up the ettringite reacts with C_4AH_{13} to form monosulphate according to the equation

$$C_3A \cdot 3C\bar{S} \cdot H_{32} + 2C_4AH_{13} \rightarrow 3C_3A \cdot CS \cdot H_{12} \text{ (monosulfate)} + 2CH + 20H \quad (7)$$

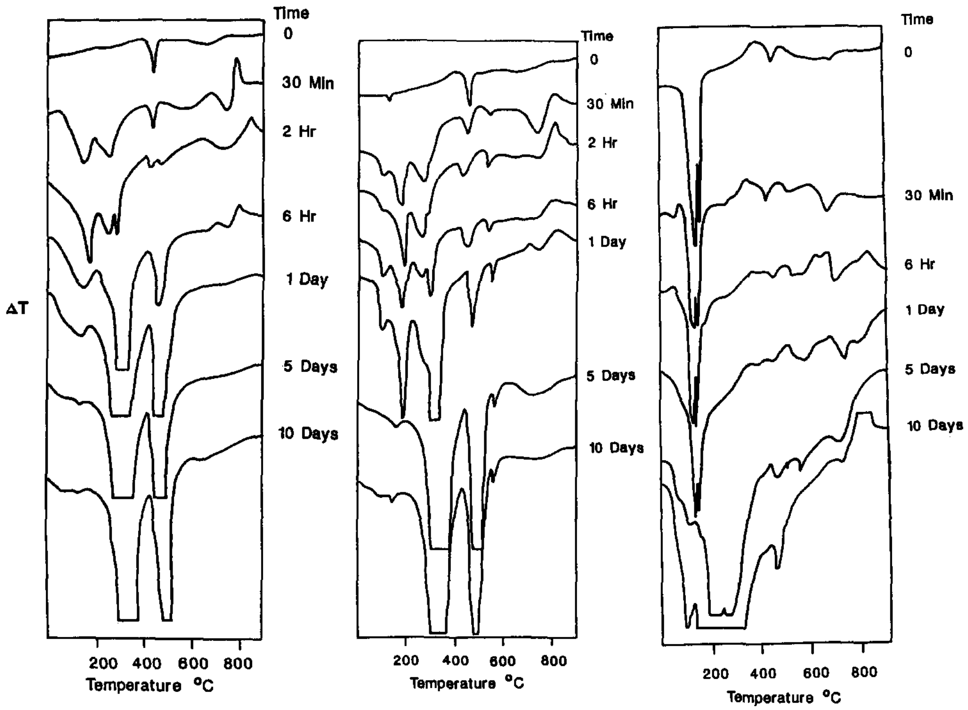

Fig. 5. DTA plots of C_3A hydrated with and without gypsum (0.25% and 20%) for 10 days at room temperature [59].

These two hydrate forms, i.e. ettringite and monosulfate, have been studied by thermal analysis for many years. Midgley and Rosaman [44] discovered the formation of a solid compound of formula between $C_3A \cdot 3CS \cdot aq$ and $C_3A \cdot 3CH \cdot aq$. Feldman and Ramachandran [59,60] have studied C_3A–gypsum mixtures containing 0.25–25% gypsum cured at 2, 12, 23 and 50 °C for up to 34 days. Typical DTA plots at room temperature are shown in Fig. 5 in which the endothermic peaks in the 170–200 °C range are attributed to ettringite. Peaks at 140–150 °C and 240–285 °C are attributed to the hexagonal hydrates C_2AH_8 and C_4AH_{13}, respectively. The compound C_4AH_{13} may also be associated with the monosulfate. The two endothermic effects at 290–300 °C and 460–500 °C are due to the cubic C_3AH_6 hydrates.

Tetracalcium aluminoferrite (C_4AF)

In the absence of gypsum, C_4AF reacts with lime and water to form iron-substituted C_4AH_{13}, which converts ultimately to a solid solution of C_3AH_6 and C_3FH_6. This reaction is more rapid at higher temperatures.

$$C_4AF + 2CH + 11H \rightarrow C_4(A,F)H_{13} \tag{8}$$

$$\xrightarrow{\approx 50\,^\circ C} (C_3AH_6 + C_3FH_6)\ \text{(solid solution)} \tag{9}$$

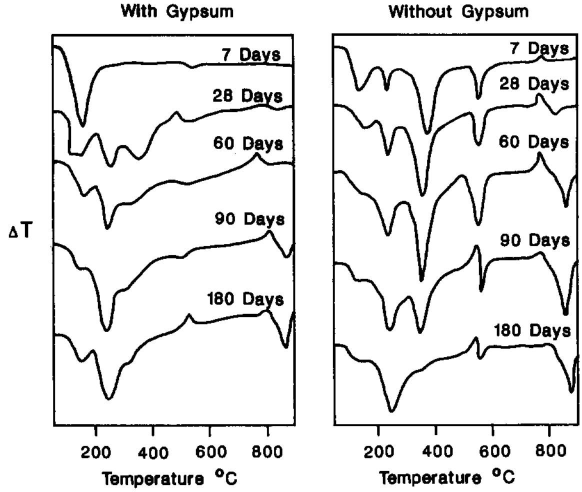

Fig. 6. DTA plots of C_4AF with and without gypsum hydrated up to 180 days at room temperature [64].

In the presence of gypsum, iron-substituted ettringite is formed as follows

$$C_4AF + 3C\bar{S}H_2 + 27H \rightarrow \underset{\text{iron-substituted ettringite}}{C_3(A,F) \cdot 3C\bar{S} \cdot H_{32}} \qquad (10)$$

When the supply of gypsum is exhausted, this ettringite transforms to iron-substituted monosulfate of the type $C_3(A,F) \cdot C\bar{S} \cdot H_{12}$.

Ramachandran and Beaudoin [12] and Collepardi and co-workers [61–63] have conducted a series of DTA investigations on the hydration behavior of C_4AF, with and without the presence of lime and gypsum. DTA plots obtained by Kalousek and Adam [64], see Fig. 6, show that a C_4AF sample hydrated for 7 days forms C_3AH_6 and C_4AH_3, corresponding to the endothermic peaks at 360 and 220 ° C respectively. The effects are maximum at 60 days and disappear after 180 days.

In the presence of gypsum, the only endothermic effect noticeable after 7 days curing is at around 150 ° C, which is most probably due to the presence of high-iron-substituted ettringite. After 28 days, two more endothermic peaks appear at around 250 and 350 ° C which are due to the formation of Al_2O_3 and Fe_2O_3 solid solutions [1]. After 90 days, the dominant endothermic peak is at around 250 ° C and is most probably due to the formation of iron-substituted monosulfates.

ACCELERATORS

The most widely used accelerator in the cement and concrete industry is calcium chloride, although a number of other compounds including formates, aluminates, sulfates, nitrates, halides, thiosulfates, carbonates and triethanolamine have also been used. Accelerators effectively increase the

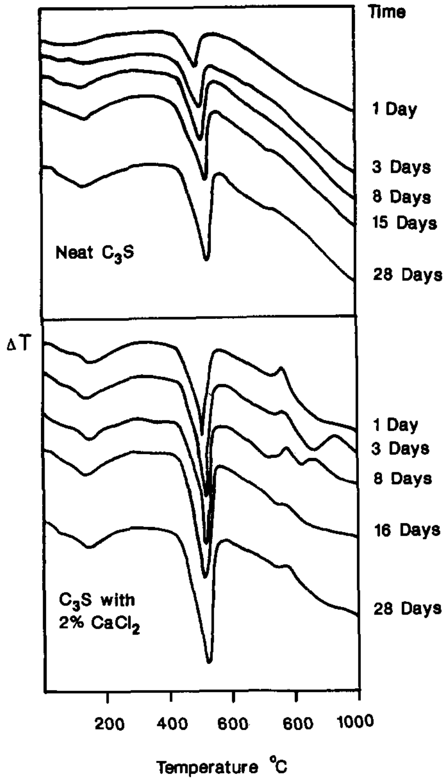

Fig. 7. DTA plots of C_3S, hydrated neat and in the presence of 2% $CaCl_2$ [14]. Hydration times are given for each plot.

rate of hydration by increasing the formation of CH in a cement paste. The rate generally increases with increasing concentration of the accelerators [58]. Because C_3S is the most abundant compound in cement, it controls the reaction kinetics of the accelerators.

Calcium chloride

C_3S

DTA techniques have been proved useful in monitoring the hydration of C_3S in the presence of calcium chloride [5,13,14,47,64–70]. Typical thermograms are shown in Fig. 7. The onset of C_3S hydration in the presence of $CaCl_2$ shows significant differences from that obtained with pure C_3S paste. The endothermic peaks below 300 °C are larger in the presence of $CaCl_2$ as compared to the neat C_3S paste. An endotherm at 550 °C appearing after 2 hours of hydration with 1% $CaCl_2$, is absent in neat C_3S paste. DTA investigations conducted by Ramachandran [65,66] and Singh and Ojha [67] also report that the hydration of C_3S in the presence of chloride shows peaks which differ from those of neat C_3S paste.

The endothermic effects due to the formation of CH seem more intense in the presence of $CaCl_2$: over 30% of the total CH formed at 30 days precipitates within 5 hours of hydration as a result of the presence of $CaCl_2$. Ramachandran [66] obtained a good correlation of DTA and TGA results for estimating the formation of CH and the rate of disappearance of C_3S with increasing additions of $CaCl_2$. The sharp exothermic peak at 690 °C after 4 hours curing, and an endothermic dip at around 820 °C, seem to be due to chloride chemisorption on the C–S–H surface and possibly also in the interlayer positions [68]. On further addition of $CaCl_2$ (up to 4%), the thermal effects become larger and more intense at earlier times than those observed with 1% $CaCl_2$.

DTA, chemical analysis and XRD studies have also revealed that $CaCl_2$ can exist in different states in the $C–CaCl_2H_2O$ system and can be so strongly held that it cannot be leached out, even with water. There is a very strong possibility that these chlorides are strongly associated in the C–S–H lattice, but the exact location and nature of this association is still unknown [68]. The chlorides might be incorporated into the C–S–H and modify its morphology. Richartz [69] verified that chloride ions entered into the C–S–H lattice formed in a C_3S phase treated with $CaCl_2$ at 80 °C under autoclave curing for longer periods. The chloride may also react with the aluminate phases, but this may vary with concentration. Additional studies showed that the C–S–H lattice formed at higher $CaCl_2$ concentrations acquires higher C/S ratios as its morphology changes from a needle-like structure to a platey structure. Midgley and Illston [70] measured the penetration of chloride ions into hardened cement pastes and worked out a correlation between water/cement ratio, porosity and chloride penetration.

Kawamura et al. [71] employed DTA techniques to study the solution composition of chloride-bearing cement pastes and mortars, with or without the presence of other additives such as fly ash. A fairly noticeable peak occurs at around 300 °C, see Fig. 8; the peak increases with time but remains unaffected by the fly ash additions.

Suzuki et al. [72] studied the effects of sodium chloride and NaOH on the formation of C–S–H in cement paste. They obtained a definite endotherm between 100 and 300 °C, ascribed mainly to the loss of weakly bound water in the C–S–H. The conversion from C–S–H to β-wollastonite is indicated by an exotherm at 850 °C. The peak temperatures, however, drops to 840 and 800 °C for C–S–H formed in NaOH and NaCl solution, respectively. Typical DTA plots for different systems are shown in Fig. 9.

C_3A

With C_3A, the $CaCl_2$ forms $C_3A \cdot CaCl_2 \cdot xH_2O$ or $C_3A \cdot 3CaCl_2 \cdot xH_2O$ aluminates, depending on the $CaCl_2$ concentration. The $C_3A \cdot CaCl_2 \cdot xH_2O$ is known as monochloroaluminate or the low-form aluminate; the $C_3A \cdot 3CaCl_2 \cdot xH_2O$ is known as high-form aluminate and forms at high $CaCl_2$

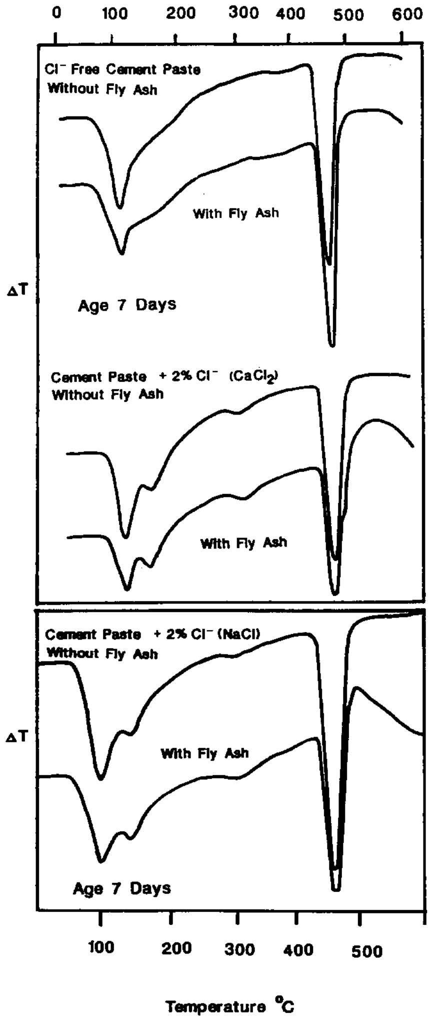

Fig. 8. DTA plots for cement pastes containing calcium chloride and sodium chloride, with or without 2% Cl and fly ash addition [71].

concentration. The compound $C_3A \cdot CaCl_2 \cdot xH_2O$ forms a series of solid solutions with C_4AH_{13}. Stukalova and Andreeva [73] have used DTA to differentiate between these two forms of aluminate. Endothermic peaks at about 190° and 350°C are indicative of the low form of aluminate, whereas the peaks appearing at around 160°C are due to the presence of high-form aluminates.

C_4AF

The effects of $CaCl_2$ on the hydration of C_4AF do not seem to differ from that on C_3A. However, there are no accounts of the application of DTA techniques on C_3A–$CaCl_2$ in the literature.

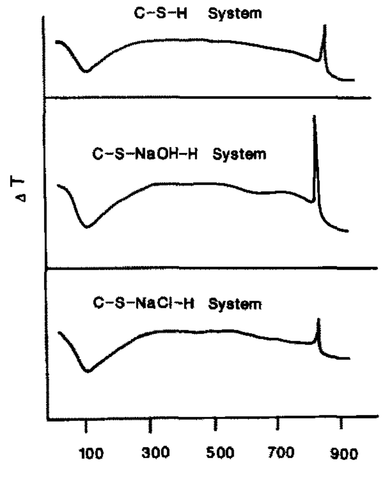

Fig. 9. DTA plots showing the C–S–H information in different (C–S–H)–chloride–alkali systems [72].

Calcium formate and other halides

One of the limitations to the wide use of $CaCl_2$ as an accelerator is its potential corrosiveness to concrete-reinforcing steel if present at high levels. Therefore, attempts have been made to find non-chloride accelerators, such as formates, halides, nitrates, sulfates, carbonates, thiosulfates and triethanolamine.

C_3S

Combined TGA, DTG and DTA studies have also been performed on cement pastes containing $CaCl_2$ together with CaF_2, CdI_2 and $CrCl_3$ as accelerators [15,67–70,73–75]. In general, the DTA plots show endothermic peaks between 450 and 550 °C due to CH dissociation.

Calcium formate also accelerates C_3S hydration [47] but is less effective than $CaCl_2$. Their comparative acceleration effects are shown as a function of CH formation in Fig. 10. The TGA plots indicate that after one day the weight loss for C_3S phase containing $CaCl_2$ is nearly 14%, compared to 4.5% for pure C_3S, 8% for C_3S containing $CrCl_3$, and 11.5% for C_3S containing $CdCl_2$. A shift in the DTA peaks also takes place with the duration of the hydration. This shift is closely associated with the degree of hydration; the higher the degree of hydration, the higher the temperature at which the CH would decompose. For a hydrating C_3S–$CaCl_2$ system, the peak at 510 °C indicates an advance stage of hydration after one day. This peak shifts to 520 °C after 28 days. The shift in peak temperature due to the presence of accelerators may also be the result of changes in the amount and morphology of the CH. According to Singh and Abha [74], in the absence of

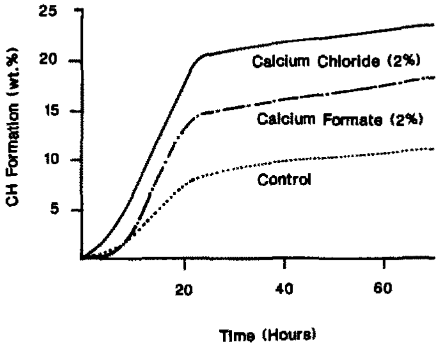

Fig. 10. Effects of $CaCl_2$ and CaF_2 on CH formation in hydrating C_3S [66].

calcium formate accelerator, the peak temperature for CH decomposition increases, whereas in the presence of an accelerator the peak temperature falls as the amount of CH being formed increases and it becomes more and more loosely packed. DTA peak temperatures of hydrated C_3S in the presence of calcium formate are given in Table 4.

A similar trend in the shift of CH decomposition temperatures with age in C_3S pastes containing $CaCl_2$, $CrCl_3$ and CdI_2 was also observed by Ben-Dor and Perez [15], who determined that although all three additives accelerate the C_3S hydration, the additional chloride ions in $CrCl_3$, as compared to $CaCl_2$ and $CdCl_2$, do not seem to have any greater effect on the hydration kinetics. Even though CdI_2 has a crystallographic structure similar to that of CH, at first, its accelerating effect is slower than that of $CaCl_2$; however, the effect is faster after 3 days, on the weight-loss basis. The plots of total weight loss against curing time for various pastes containing different

TABLE 4

DTA peak temperatures of hydrated C_3S in the presence of CaF_2 [74]

Time of hydration (h)	Conc. of calcium formate (%)	DTA peak temperature (°C)
8	0	560
16		570
24		580
8	2	570
16		580
24		590
16	4	580
24		580
16	6	580
24		580

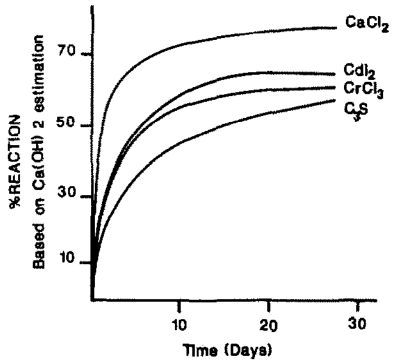

Fig. 11. Percent reaction based on estimation of CH content vs. hydration time for C_3S pastes treated with different accelerators [13].

accelerators are shown in Fig. 11. Acceleration generally lowers the CH peak temperatures; however, with age, the peak temperatures increase as the CH becomes more and more compact. Optimum shifts in peak temperatures for all the accelerators is reached in eight days. Typical plots of peak shifts against hydration times are shown in Fig. 12.

Thiosulfates and nitrates

C_3S

Calcium thiosulfate, CaS_2O_3, and calcium nitrate, $Ca(NO_3)_2$, can also accelerate the hydration of C_3S phase. Murakami and Tanaka [76] studied the accelerating properties of both CaS_2O_3 and $Ca(NO_3)_2$ (each 3% by weight) using DTA techniques; their plots are shown in Fig. 13. The endotherm below 200 ° C is due to C–S–H decomposition, and the peaks around 550 ° C are due to CH decomposition. The small peak before the larger 500 ° C peak is most probably due to amorphous CH. The exothermic effects in the presence of $CaCl_2$ and CaS_2O_3 could be due to any chemisorbed complex being formed with the C–S–H phase [65].

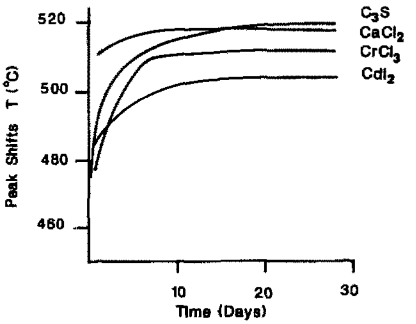

Fig. 12. CH peak shifts in C_3S hydration with addition of 2% $CaCl_2$, CrCl and $CdCl_2$ [13].

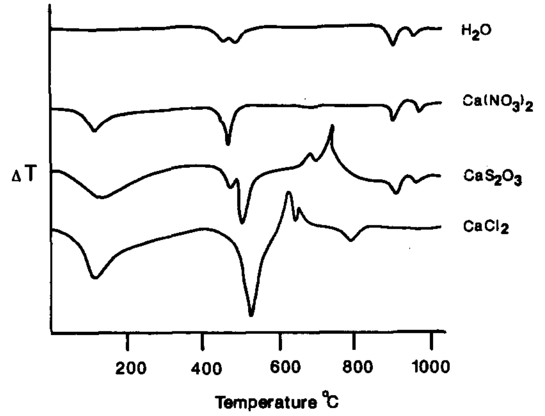

Fig. 13. Thermograms of C_3S and its hydration products in the presence of different calcium salts [65].

C_3A

The DTA thermograms of C_3A hydrating in the presence of CaS_2O_3, $Ca(NO_3)_2$ or $CaCl_2$ are different. The presence of thiosulfates and chlorides result in the formation of C_2AH_8 and other complex hexagonal products of composition $C_3A \cdot Ca(OH)_2 \cdot xH_2O$; or of hydration products in which Cl^- and $S_2O_3^-$ are substituted is the structure [65]. With $Ca(NO_3)_2$, however, cubic C_3AH_6 is formed.

Carbonates

C_3S

According to Ramachandran [77], carbonates such as $CaCO_3$ also accelerate the C_3S hydration. DTG plots of C_3S hydrating in the presence of $CaCO_3$ show three inflections at 100–120 °C, 460–475 °C and 730–740 °C, due to water loss from C–S–H, dehydration of CH and decomposition of $CaCO_3$, respectively. The acceleration effects are greater for larger additions of carbonates, and for smaller $CaCO_3$ particle size. As with the C_3S–$CaCl_2$ system, there could also be the possibility of complex formation between $CaCO_3$ and the hydrating C_3S [77].

C_3A

$CaCO_3$, $MgCO_3$, and a combination of $CaCO_3$ and $MgCO_3$ also act as accelerators for hydrating C_3A [78]. They react with C_3A to form a carboaluminate complex of composition $3CaO \cdot Al_2O_3 \cdot CaCO_3. 11H_2O$. Thermograms of hydrating C_3A in the presence of different carbonates for 28 days are shown in Fig. 14. Neat C_3A paste exhibits two endothermic effects: i.e. a pronounced peak at 300 °C and a broad endotherm at about 450 °C, which are both typical of the presence of cubic phase C_3AH_6. In the presence of

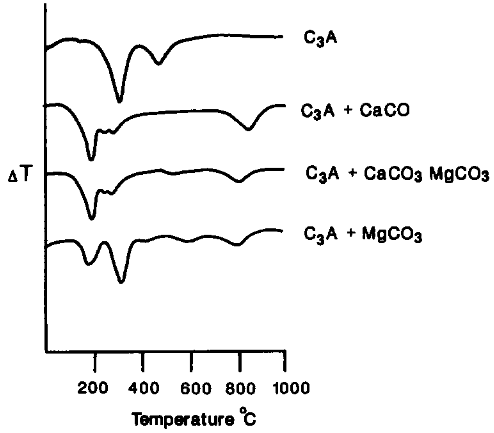

Fig. 14. Thermograms of C_3A hydrated for 28 days with carbonate admixtures [65].

$CaCO_3$, and a $CaCO_3$–$MgCO_3$ combination, large endotherms at 200 °C and very small endotherms at 300 °C are observed. With $MgCO_3$, a sharp peak at 300 °C is observed which is indicative of the presence of a large amount of C_3AH_6. Peaks at 200 °C correspond to the formation of a complex primarily composed of carboaluminates.

Triethanolamine (TEA)

C_3S

The effects of another type of accelerator, triethanolamine (TEA), on the hydration of C_3S phase were investigated by Ramachandran [66]. The presence of endothermal peaks in the range 480–500 °C are caused by the formation of CH. Decomposition takes place after about 10 hours when 0.5% TEA is used. The peaks at 480–500 °C grow larger with hydrating time. Figure 15 shows the thermograms of C_3S containing TEA hydrated for 28 days.

Mono- and diethanolamine exhibit an acceleration behavior with respect to C_3S hydration, that is similar to that of TEA.

C_2S

TEA may also act as a retarder to the C_2S phase, resulting in two endothermic peaks at 480–500 °C. The higher temperature peaks may be ascribed to the formation of both crystalline and non-crystalline CH. The effects of TEA on C_2S hydration show a similar trend, see Fig. 16. The endothermal peaks reveal some twin effects which correspond to the possible formation of an amorphous type of CH [65].

C_3A

Ramachandran [7] has also studied the effects of TEA on hydrating C_3A, with or without the presence of gypsum. Without gypsum, TEA accelerates

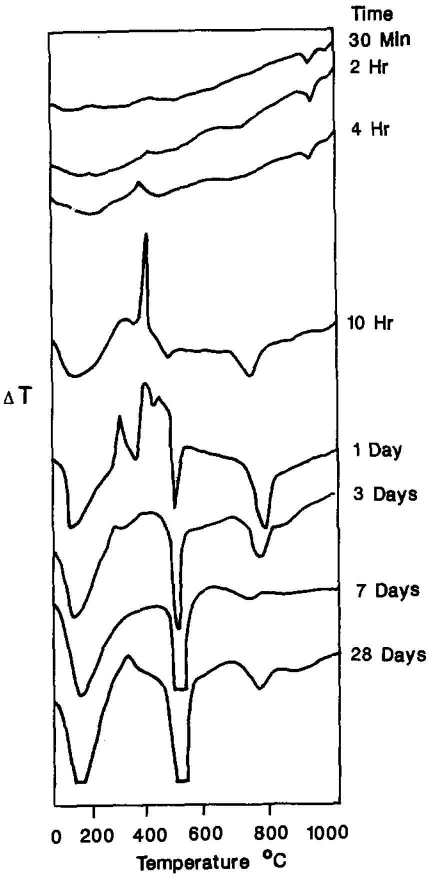

Fig. 15. DTA plots of hydrated C_3S in the presence of 0.5% TEA [66].

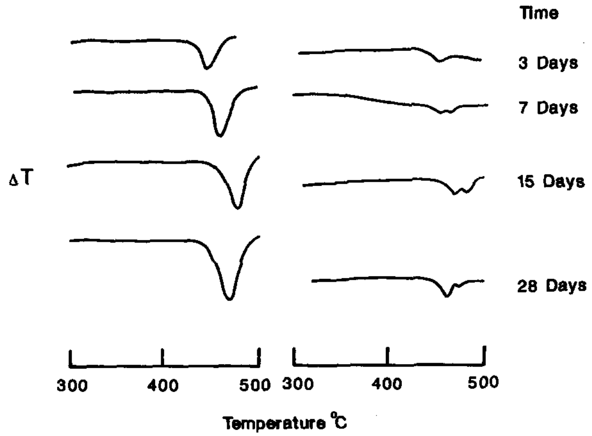

Fig. 16. DTA plots of C_2S hydrated with TEA [65].

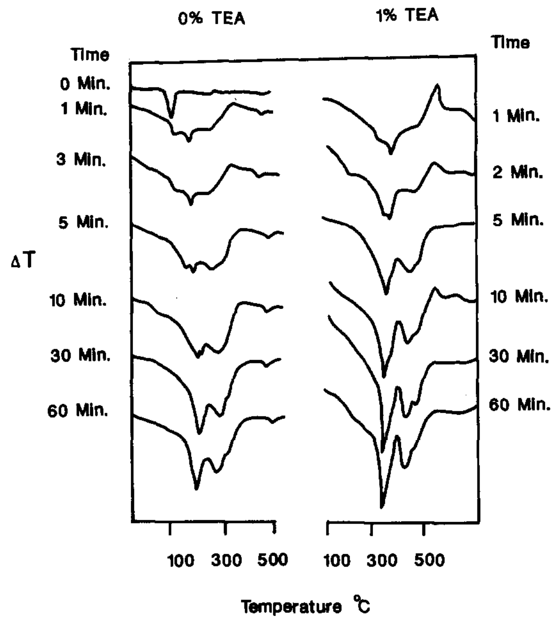

Fig. 17. DTA plots of $C_3A + 5\%$ gypsum mixture hydrated with and without 1% TEA [7].

C_3A hydration, as observed from the intensification of the peaks at 150 °C and 250 °C, due to the formation of hexagonal C_2AH_8 and C_4AH_{13}, respectively. With gypsum addition, the formation of ettringite is accelerated. The endotherm at 170 °C and the twin peaks between 250 and 300 °C, as shown in Fig. 17, are developed due to the formation of hexagonal hydrates and the conversion product with monosulfate. The accelerating effects increase with increasing concentrations of TEA.

Oxalic acid

With oxalic acid as the accelerator in the cement paste, the DTA plots give different endothermic peaks at 300, 480, 550 and 620 °C that could be associated with the existence of calcium oxalates [65].

WATER REDUCERS/RETARDERS

One of the generally accepted explanations of the effects of water reducers/retarders on cement paste is that they chemisorb either on the highly reactive components, C_3A and C_3S, or on the nuclei of their hydration products which poisons their growth. It should be pointed out that C_3A the most reactive compound although present in small amounts, plays a significant part in the early setting behavior of cement. That is why the bulk of the published analytical work in this field, including thermal analysis, refers most frequently to C_3A–retarder systems; hence, this is reviewed in more detail in the following sections.

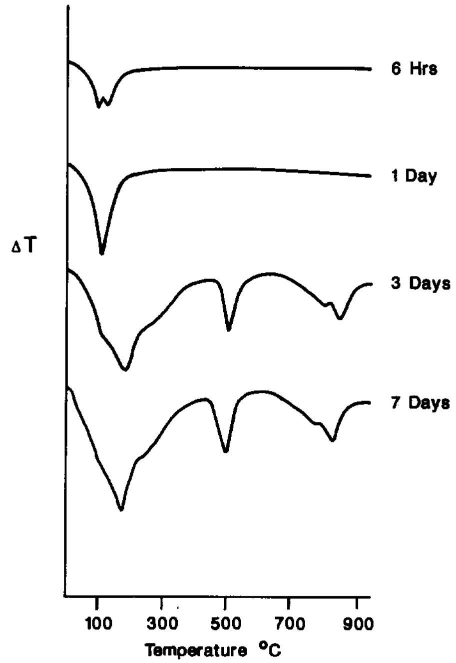

Fig. 18. DTG plots showing the influence of sugar-free sodium lignosulfonate (0.3%) on hydrated paste of $C_3S(76\%)+C_3S(19\%)+\text{gypsum}(5\%)$ [97].

Lignosulfonates

Cement paste containing lignosulphonates (both sugar-free and commercial) show endothermic peaks at 450–500 °C resulting from the dehydration of CH. The intensity of these peaks indicates the extent of hydration of the C_3S component. Relatively lower peak areas of CH decomposition in DTG plots for a paste containing 76% C_3S, 19% C_3A and 5% gypsum, hydrated with sugar-free sodium lignosulfonate for different hydration periods, suggest similar retarding effects on hydration (Fig. 18). Thermograms of C_3S and C_3A hydrated with sugar-free lignosulfonates show similar retarding effects.

C_3A

Adsorption data collected by Young [79] has shown that C_3A, as compared to the other phases in cement such as C_3S and C_2S, adsorbs the maximum amount of lignosulfonate. Therefore the adsorption of lignosulfates on aluminates is primarily responsible for the retarding action on cement pastes. Young [79] also observed changes in the hydration products of C_3A in the presence of lignosulfonates using thermal analysis, X-ray diffraction and microscopy. Numerous workers [58,65,79–98] have used DTA to study the effects of lignosulfonates and other retarders based on

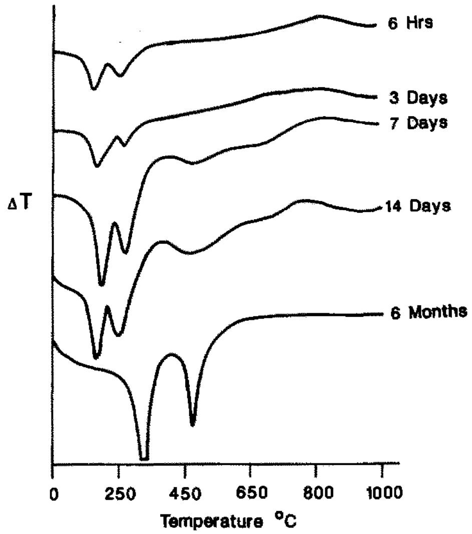

Fig. 19. DTA plots of C_3A containing calcium lignosulfonate [65].

sugars and hydroxycarboxylic acids, on the hydration of different cement phases. Ramachandran [80] and Tenoutasse and Singh [81] used thermoanalytical and microcalorimetery, combined with DTA and X-ray diffraction respectively, to study cement systems in the presence of lignosulfonates and other sugars.

Some of the DTA plots obtained by Ramachandran [65] for C_3A compound hydrated for different periods are shown in Fig. 19. The plots show two distinct endothermic peaks in the ranges 150–200 °C and 200–280 °C. These peaks are indicative of the presence of hexagonal phase and increase with hydrating time. The cubic phase shows two endotherms at about 300–350 °C and 500–550 °C and becomes increasingly stable at 14 days when the endotherms just begin to appear. Cubic C_3AH_6 appears as a main phase at 6 months as is evident from the endotherms. The peaks become intense with hydration which infers that the lignosulfonate stabilizes the hexagonal hydrates C_4AH_{13} and C_2AH_8 with respect to C_3AH_6.

Ramachandran and Feldman [65,82] conducted combined adsorption–desorption and XRD studies to elucidate the effects of calcium lignosulfonate on the C_3A, C_4AH_{13}, C_2AH_8 and C_3AH_6 phases, and concluded from strong irreversible isotherms that a substantial amount of lignosulfonate was adsorbed on the hexagonal phases. This also implies that the lignosulfonate enters the interlayer region of the hexagonal phases, particularly C_4AH_{13}, and form certain complexes that stabilize them with respect to the cubic C_3AH_6. They also observed the complex effects that result when C_3A is treated with calcium lignosulfonate in excess of 10%; this also produces thermograms different from those of lignosulfonates or aluminum hydrate.

TABLE 5

Estimation of various phases formed in the C_3A–lignosulfonate–water system [82]

Starting systems	Hydrating periods			
	6 h	3 days	7 days	6 months
C_3A–H_2O	C_3A C_2AH_8 C_4AH_{13}	C_3A C_2AH_8 C_4AH_{13} C_3AH_6	C_3A C_3AH_6	C_3AH_6
C_3A–lignosulfonate–H_2O	C_3A C_2AH_8 C_4AH_{13}	C_3A C_2AH_8 C_4AH_{13}	C_3A C_2AH_8 C_4AH_{13}	C_3AH_6

The retarding effect of lignosulfonate in cement is mainly attributed to the larger adsorption effects of lignosulfonates on the C_3A phases in aqueous phase [82]. The adsorption values are reported to be in the order $C_3A > C_4AF > C_3S > C_2S$ [98]. The effects on C_3A may also depend on the alkali content of the cement. Lignosulfonates are less effective in cements with high C_3A and alkali contents [83]. Ramachandran suggests that high alkali contents may reduce plasticizing ability by interacting with lignosulfonates [84]. Collepardi and co-workers [85,86] employed DTG techniques to monitor the retardation behavior of sodium lignosulfonate–alkali–carbonates–C_3A systems. The peaks between 100 and 300 °C indicated the effects of retardation. They found that the combination of sodium carbonate and sodium lignosulfonate (1.25% each) was more effective a retarder than sodium lignosulfonate for C_3A hydration in the presence of $Ca(OH)_2$. Jawed et al. [38] obtained similar results using conduction calorimetry.

In the presence of calcium lignosulfonate, C_3A converts on hydration to a hexagonal hydrate and then, more slowly, to cubic hydrates [82]. Typical results are shown in Table 5. The degree of conversion depends on the lignosulfonate concentration, the hydration temperature and the time of contact. Thermograms of the products formed in the C_3A–calcium lignosulfonate–H_2O systems containing increasing amounts of lignosulfonate (up to 20%) are shown in Fig. 20. The thermogram of the hexagonal phase exhibits an intense exothermic peak at 790 °C and an endothermic effect at 825 °C. The exothermic peak is attributed to the oxidation of strongly bound lignosulfonates on the hexagonal phase. At concentrations above 50%, a dark brown gel begins to form as a deposit on the heavier whiteish mass originally present. At higher concentrations, the distinction between these two masses becomes more evident.

Ramachandran and Feldman's [65,82] investigations into the retarding effects of lignosulfonates on the C_2AH_8 and C_4AH_{13} suspensions using DTA and adsorption–desorption isotherms, were later verified by Massazza

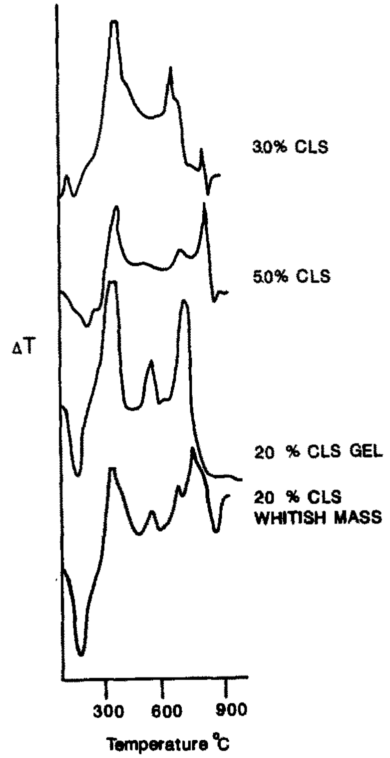

Fig. 20. DTA plots of products formed in the C_3A–calcium lignosulfonate–water systems at different lignosulfonate concentrations [82].

et al. [87] who studied C_4A_{13}–lime dispersions. In both studies the isotherms showed a rapid increase in adsorption, tapering off towards equilibrium concentrations. DTA studies by Ramachandran and Feldman [88] had earlier suggested that an interlayer complex forms between the lignosulfonates and C_2AH_8 and C_4AH_{13}, which stabilizes them with respect to their conversion to cubic C_3AH_6. Later studies by Ramachandran and Feldman [65,82] found no significant difference caused by the addition of calcium lignosulfonate to the C_3AH_6. Figure 21 shows a thermogram of the products formed in the hexagonal phase–calcium lignosulfonate–H_2O system. Sharp peaks at around 360 °C are common in the plots given in Figs. 20 and 21. The main difference is a large endothermic peak at 100 °C and an endothermic peak at 730 °C which is hardly noticeable for the plot of calcium lignosulfonate in air. The DTA results for cubic C_3AH_6 treated with lignosulfonate show strong peaks in both air and nitrogen (Fig. 22). The sharper peaks for C_3AH_6 containing lignosulfonates are due to their fine particles.

Young [79] used DTA to study the influence of lignosulfonate on the hydration of the C_3A–gypsum–lime system, and found that the initial

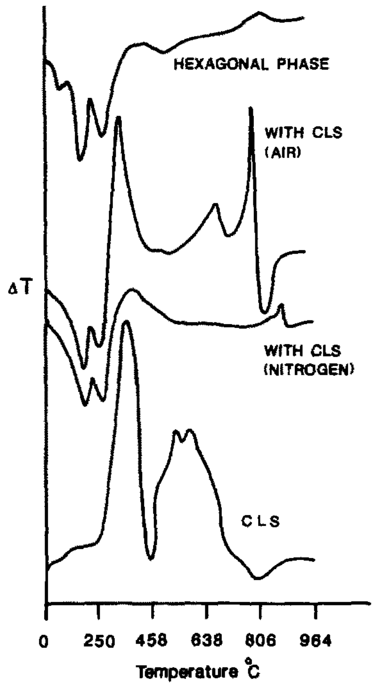

Fig. 21. TDA plots of products formed in the hexagonal-phase–lignosulfonate–water system [65].

acceleration reaction between C_3A and gypsum was very slight. Instead, a noticeable retardation effect was observed. Ettringite was recognized within minutes of addition of the admixture, whereas the conversion of ettringite to

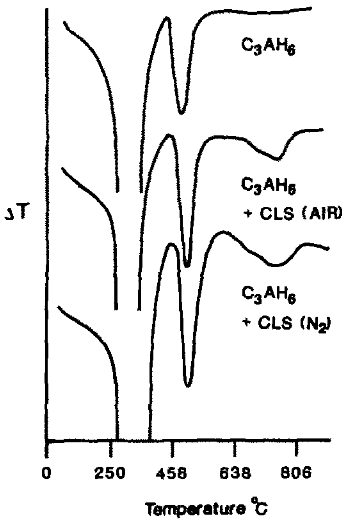

Fig. 22. DTA plots of the cubic phase treated with lignosulfonate [82].

monosulfonate took place in 3 days as compared to 3 hours without the addition. Massazza and Costa [89] used TG, DSC, XRD and calorimetric techniques to confirm this; although lignosulfonates slightly retard the C_3A–gypsum reaction, the transformation of ettringite to monosulfonate is significantly retarded. Lignosulfonates also modify the morphology of ettringite, C_2AH_8, C_4AH_{13} and the monosulfonate, when consumed by the C_3A.

Pauri et al. [86] studied the combined effects of sodium lignosulfonates and Na_2CO_3 on C_3A hydration. They observed that the liquifying effects of these admixtures were due to a strong retarding action that results in a change in zeta-potential and noticeable dispersion effects. They substantiated their TG and DTG results with XRD analysis.

C_3S

Monosi et al. [93] used DTG and TG curves to establish that 0.3% sodium lignosulfonate and/or carbonate almost completely inhibits the hydration of C_3S alone or in the presence of C_3A for 14 days. The combined effects of Na_2CO_3 and lignosulfonate strongly retard the C_3A hydration. However, mixing with 20% C_3A decreases the retardation slightly. Ramachandran [80] found similar results using conduction calorimetry. Milestone [94] and Young [95] also arrived at similar conclusions from their studies on the retarding effects of lignosulfonates and sugar acids on C_3S alone and with up to 5% C_3A addition. Figure 23 shows the DTG curves obtained by Monosi et al. [93] for C_3S hydration with and without sodium lignosulfonate. Milestone [94] also discussed the retarding effects in terms of poisoning of the nucleation sites and found that in the presence of 0.1%

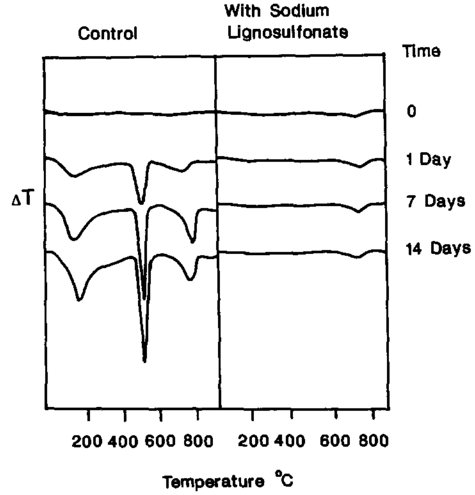

Fig. 23. DTG plots of C_3S hydration with and without addition of sugar-free sodium lignosulfonate [93].

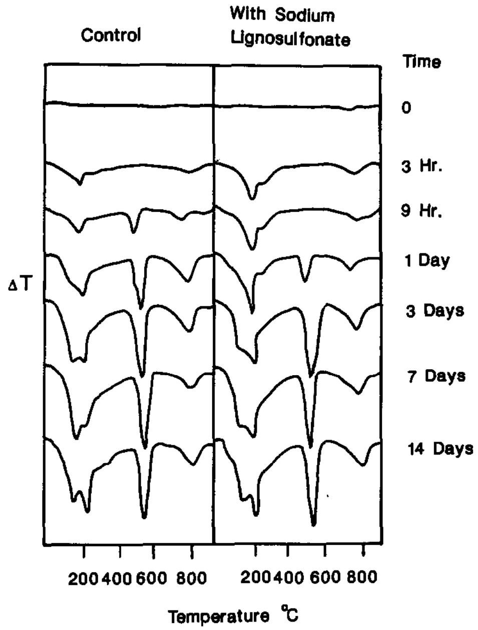

Fig. 24. DTG plots of $C_3S:C_3A$ hydration in the presence of sodium lignosulfonate [93].

calcium lignosulfonate and other sugar-based retarders such as glucose and sodium gluconate, the C–S–H forms as flaky particles covering the amorphous CH.

An adsorption–desorption isotherm of lignosulfonates on fully hydrated C_3S shows initially a rapid irreversible adsorption, probably onto the interlayer position. The irreversibility becomes intense as the concentration of lignosulfonate increases. Ramachandran [6] has made use of thermal analysis to explain the adsorption on the $C_3S–H_2O$ system doped with lignosulfonates; according to Ramachandran, an exothermal DTA peak at 800 °C confirms the formation of an interlayer complex between the C–S–H and the lignosulfonates.

In a $C_3S–C_3A–H_2O$ system without gypsum, the C_3A may act as a sink for lignosulfonates [6,69,99–101]. The DTG plots in Figs. 23 and 24 show a comparison of the influence of sodium lignosulfonate (0.3%) on the C_3S hydration alone and in the presence of C_3A. Lignosulfonates block completely the C_3S hydration for up to two weeks in the absence of C_3A. In the presence of C_3A, the blocking is only for one day. Addition of C_3A seems to destroy the retarding effect of the lignosulfonates on C_3S [6,65,96]. At lower C_3A contents and larger lignosulfonate concentrations, the retarding effects on C_3S are for longer periods, and vice versa [95]. An effect of the combination of sodium lignosulfonates and sodium, carbonate on the C_3S hydration in the presence of C_3A, is similar to that of lignosulfonate, except that complete inhibition occurs for only 30 minutes, as shown in Fig. 25.

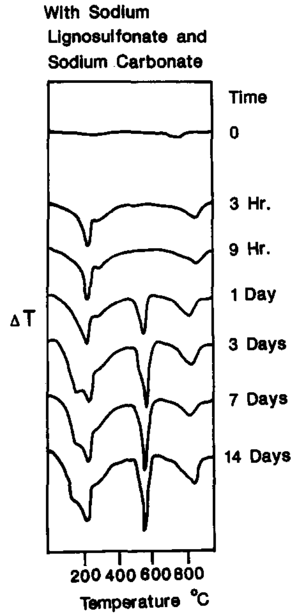

Fig. 25. DTG plots of $C_3S:C_3A$ hydration in the presence of sodium lignosulfonate and sodium carbonate [93].

C_2S

Lignosulfonates (and other retarders such as salycylic acid) also retard C_2S hydration but in the presence of C_3A the retardation is less effective than for the C_3S phase [97]. C_3A again acts as a sink for lignosulfonate, and leaves less admixture for C_2S retardation. Thermal data on the retardation of C_2S are not available.

C_4AF

The C_4AF phase adsorbs much less retarder than does C_3A. The hydration products, being amorphous, are easily detected by DTA and DTG [53]. Collepardi et al. [62] determined that the combined effect of 2.5% sugar-free sodium lignosulfonate and sodium carbonate retards the C_4AF hydration for up to one day. The higher the concentration of the admixture, the larger the induction period. Moreover a sharp change in zeta-potential, caused by the simultaneous addition of lignosulfonate and carbonates, explains the liquifying effects that result from their addition. Figure 26 shows the weight losses in the TGA plots as an indication of C_4AF retardation.

Lorprayon and Rossington [58] noted that in the presence of calcium lignosulfonate the microstructure of the C_4AF hydration products remain unchanged for ten minutes. The DTA plots (Fig. 27), however, indicate the formation of small amounts of C_2FH_8, C_4FH_{13} and C_3FH_6, mostly with an amorphous nature; after 60 minutes, thin hexagonal plates do appear.

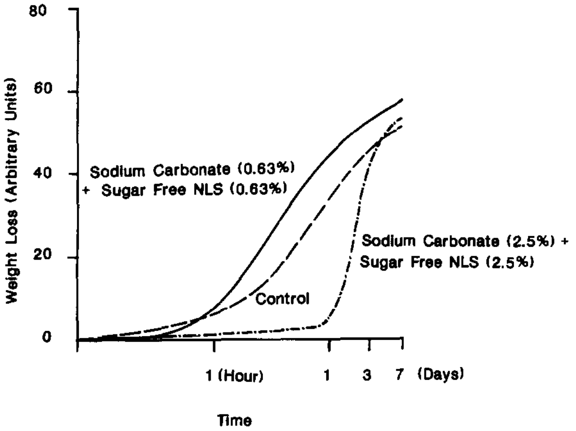

Fig. 26. Effects of sodium carbonates and sugar-free sodium lignosulfonate mixture on C_4AF hydration [62].

Sugars and their oxidation products

C_3A

The retarding action of sugars and their oxidation products on C_3A hydration as determined by DTA is well documented by Ramachandran [65], Young [90] and Milestone [91]. Figure 28 shows the influence of 1% each of sucrose and trehalose on C_3A hydrated for 90 days. The three endothermal effects at around 100 and 200 °C are due to the formation of a

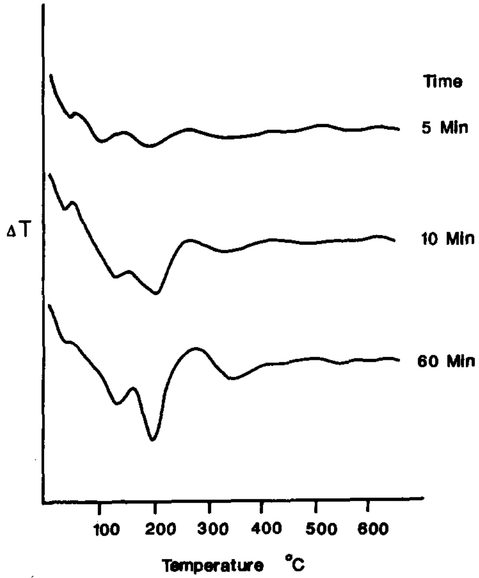

Fig. 27. DTA plots for C_4AF with lignosulfonate [58].

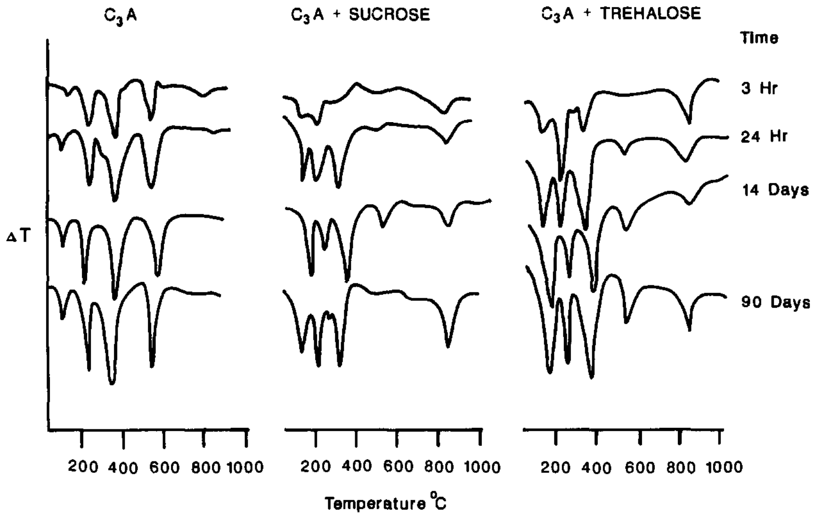

Fig. 28. DTA plot C_3A with 1% sucrose and trehalose [65].

mixture of hexagonal hydrates; the peaks at 300–350 °C are due to the cubic hydrates. Without sugars, C_3A shows a sharp peak at 550 °C at 3 hours due to early formation of cubic hydrate. With sucrose, this peak is missing even after 90 days, whereas with trehalose, this peak is present though somewhat less strong than for pure C_3A, indicating the presence of cubic phase after relatively shorter hydrating times.

Milestone [91] determined the formation of hexagonal and cubic complexes in C_3A phase retarded with 1% glucose and some of their oxidation products, such as calcium gluconate or glucuronic acid. Retardation was more effective at higher concentration. Calcium gluconate, being more stable in the alkaline conditions, was a stronger retarder than glucose or glucuronic acid at a given concentration The results show that the hexagonal hydrate C_4AH_{13} is stabilized with respect to cubic C_3AH_6. Typical results are given in Table 6; they indicate that the C_3A hydration with calcium gluconate is 18% compared to 85% with glucose; and there is no conversion to cubic C_3AH_6, even after 28 days, as compared to 3 days for glucose. The DTA peaks at 80 °C for C_3A pastes doped with calcium gluconate and glucuronic acid (0.1% for 7 days) and glucose (1% for 28 days), the endothermic peak at 200 °C and a large exothermic peak at 400 °C for calcium gluconate (1% for 28 days), as shown in Fig. 29, also confirm the existence of such complexes [91,92].

C_3S

The effects of glucose, sodium gluconate and, also, of sugar-free lignosulfonates, on a C_3S(79%)–C_3A(19%)–gypsum(5%) system show that the formation of CH is inhibited for one day by lignosulfonate or gluconate, and

TABLE 6

XRD identification of various phases formed in the C_3A pastes treated with glucose, calcium gluconate and glucuronic acid (0.1 wt.%) [92]

Admixture	% C_3A hydrated in 28 days	Hydrating time (days)			
		1	3	7	28
Glucose	85	C_3A C_4AH_{13} C_3AH_6	C_3AH_6 C_3A C_4AH_{13}	C_3AH_6 C_3A C_4AH_{13}	C_3AH_6 C_3A C_4AH_{13}
Calcium gluconate	18	C_3A	C_3A C_4AH_{13}	C_3A C_4AH_{13}	C_3A C_4AH_{13}
Glucuronic acid	20	C_3A	C_3A C_4AH_{13}	C_3A C_4AH_{13}	C_3A C_4AH_{13}

for three days by glucose, as shown by the DTG plots in Fig. 30. Thus the retarding effectiveness of these admixtures decreases in the order glucose > gluconate > lignosulfonates. Both glucose and gluconate most probably stabilize the formation of ettringite with respect to its conversion to monosulfonate.

Milestone [94] studied the interaction of C_3S with certain retarders including glucose and sodium gluconate and detected that the morphology of the C–S–H gel in their presence is in the form of flakes covering the C_3S and amorphous CH. In the later stages, however, the C–S–H becomes

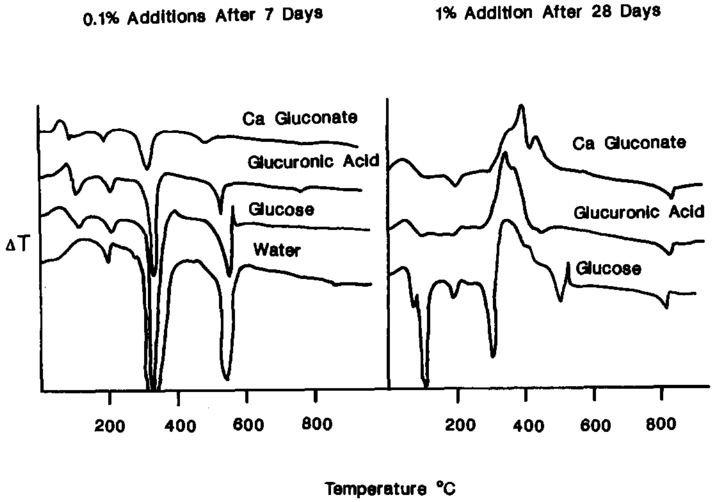

Fig. 29. DTA effects of gluconate, glucuronic acid and glucose on the formation of interlayer complexes during C_3A retardation [91].

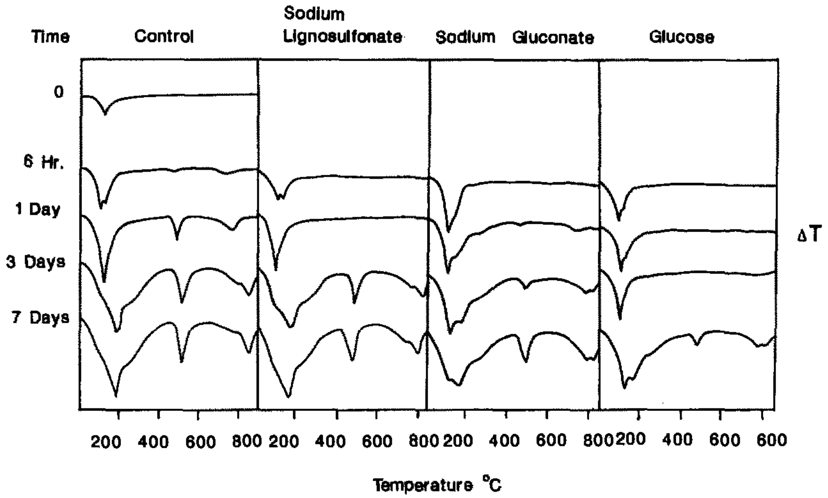

Fig. 30. DTG plots of the C_3S+C_3A+gypsum system in the presence of sugar-free lignosulfonate, glucose and gluconate [97].

acicular and the CH becomes crystalline, and are, thus, easily detected by both XRD and DTA.

Hydroxycarboxylic acids

C_3A

Organic retarders based on hydroxycarboxylic acids retard the C_3A hydration by inhibiting the conversion of hexagonal C_2AH_8 and C_4AH_{13} to C_3AH_6, most probably through complex formation.

Lorprayon and Rossington [58] studied the effects of salicylic acid on the hydration of various cement constituents at 20 : 1 water to cement ratio, and compared the results to those obtained with lignosulfonates. They also studied the effects of these admixtures on the morphological changes of the hydration products, using XRD along with DTA techniques. They estimated that with addition of lignosulfonate in the C_3A phase the main products were C_2AH_8 and C_3AH_6, while with salicylic acid they were mainly C_2AH_8 and C_4AH_{13}.

According to Bruere [102], delaying the addition of retarders makes them generally more effective. Otherwise, at lower concentration the retarders may act as accelerators. Singh et al. [99] observed a similar accelerating behavior in cement pastes doped with lactic acid. By employing DTA technique, they confirmed an increase in the C–S–H peak area between 500 and 600 °C with a concentration of lactic acid for a given hydration time (see Fig. 31).

Milestone [103] used DTA to identify retarders before use, to avoid any possibility of adverse reactions during hydration. He demonstrated that the

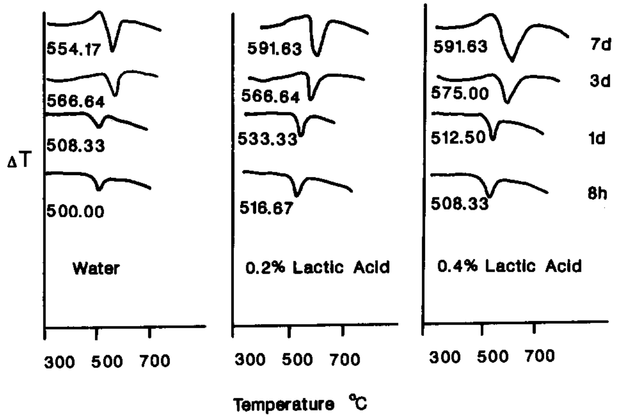

Fig. 31. DTA plots for hydrated cement paste in the presence of lactic acid [99].

retarders containing lignosulfonates and sugars display an exotherm between 200 and 400 ° C, while those containing hydroxycarboxylic acid groups show an exothermic peak between 500 and 700 ° C. Typical DTA plots for these classes of retarders are shown in Fig. 32.

Gupta and Smith [100] also conducted investigations on the thermoanalytical aspects of certain concrete admixtures containing salts of lignosulphonates, gluconates and melamine formaldehyde condensates. The ef-

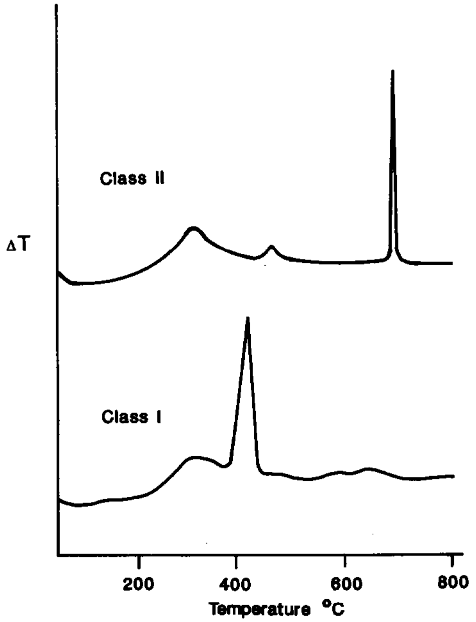

Fig. 32. DTA plots for admixtures based on lignosulfonate (Class I) and hydroxycarboxylic acid (Class II) [103].

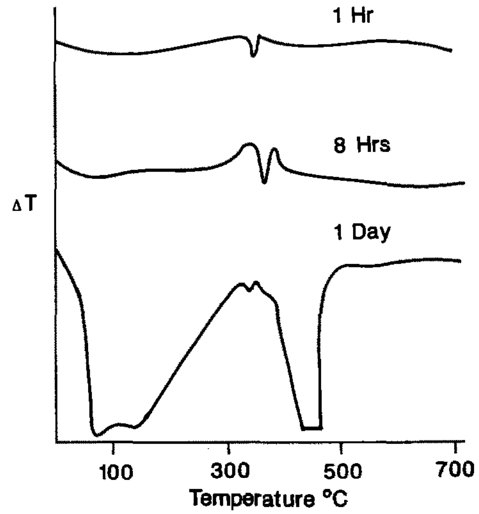

Fig. 33. DSC curves for C_3S hydrated in the presence of sulfonated melamine formaldehyde [66].

fects of hydration rates and purging gas atmosphere on their thermal properties were observed, and supplementary information was obtained from infrared spectroscopy.

SUPERPLASTICIZERS

Ramachandran [66] confirmed that sodium salts of sulfonated melamine formaldehyde condensate (SMF) retard the hydration of C_3A and C_3S. However, it accelerates the formation of ettringite in a C_3A–water system with added gypsum. DSC curves for C_3S phase hydrated in the presence of SMF for 1, 8 and 24 hours are shown in Fig. 33. It seems that the formation of CH in the C_3S–SMF system does not start at 8 hours. There is, however, evidence of CH formation after 24 hours of hydration.

The mechanism of the action on concrete samples of some admixtures based on naphthalene sulfonate formalin condensate was studied by Dezhen et al. [101] using DTA along with X-ray diffraction and infrared techniques. Their studies were based on estimation of the water formed during different stages of the hydration.

AIR-ENTRAINERS

DTA data on the effects of air-entraining agents on cement hydration are not available. However the heat evolution curve of cement paste is modified in the presence of certain air-entraining agents. For instance, according to Kreiger [104], air-entraining agents based on ethyloxylates have little effect on the heat of hydration curve. Agents based on sulfates or sulfonates retard the C_3S peak and accelerate the C_3A peak, sometimes splitting it into two. Salts of fatty acids, such as sodium oleates, accelerate the C_3A peak-splitting, but the C_3S peak remains unaffected. Most probably, calcium oleate–aluminate hydrate is formed, which retards the formation of ettringite and its subsequent conversion to monosulfate.

ANTIFREEZES

The application of an antifreezing admixture is beneficial in winter concreting and allows conservation of heat and electrical energy. Antifreeze admixtures are used extensively in regions where the air or ground temperature remains between +5 °C and −30 °C [105]. Antifreezing admixtures either lower the freezing point of the liquid phase, or accelerate the setting of cement with good antifreeze characteristics. Sodium chloride, sodium nitrite, calcium chloride, mixtures of calcium chloride and sodium chloride, and calcium nitrite–nitrate with the addition of urea, if required, are the most commonly used antifreeze admixtures. In milder climates where the temperature does not go below −10 °C, carbamides are used successfully. Carbamides can also be used in combination with other admixtures containing calcium nitrate–nitrite and urea.

Admixtures based on calcium chloride, nitrite and nitrate accelerate the hydration of C_3S and C_2S by promoting the nucleation and crystallization of their hydrates [106]. Carbamides form complex salts with the CH produced from the silicate hydrates, thus increasing the metastability and solubility of the phase resulting in increased hydration. CH also forms hydroxysalts with the admixtures and promotes densification of the resulting microstructures of the cement pastes.

The aluminate and aluminoferrite phases, i.e. C_3A and C_4AF form slightly soluble, hydrated double salts with the antifreezing agents.

Data on the application of thermal analysis techniques to monitor the effects of antifreezing agents on cement hydration are not available.

CONCLUSIONS

Thermoanalytical techniques are rapidly achieving immense importance in the study of cement and its chemical admixtures. The techniques are fast and reliable and can detect the minor physicochemical changes that occur during the hydration process of individual cement phases in the presence of given admixtures or a combination of admixtures. The techniques often provide additional information not readily available from other analytical methods. However, the results and interpretations of thermoanalytical techniques can be readily substantiated by those of other techniques such as conduction calorimetry, X-ray diffraction, scanning electron microscopy, adsorption–desorption isotherms and chemical analysis.

REFERENCES

1 V.S. Ramachandran, Application of Differential Thermal Analysis in Cement Chemistry, Chemical Publishing Company, Inc., New York, 1969.
2 R. Barta, in R.C. Mackenzie (Ed.), Differential Thermal Analysis, Vol. 11, Academic Press, London, 1972, p. 207.
3 R.C. Mackenzie, in Taylor (Ed.), The Chemistry of Cements, Vol. 2, Academic Press, London, 1964, p. 271.
4 L. Ben-Dor, in A. Ghosh (Ed.), Advances in Cement Technology, Pergamon Press, Exeter, UK, 1983, p. 673.
5 V.S. Ramachandran, Cem. Concr. Res., 9 (1979) 677.
6 V.S. Ramachandran, Cem. Concr. Res., 2 (1972) 179.
7 V.S. Ramachandran, Cem. Concr. Res., 3 (1973) 41.
8 V.S. Ramachandran, Calcium Chloride—Science and Technology, Applied Scientific Publication, U.K., 1976.
9 V.S. Ramachandran and R.F. Feldman, Cem. Concr. Res., 3 (1973) 729.
10 V.S. Ramachandran and R.F. Feldman, J. Appl. Chem. Biotechnol., 23 (1973) 625.
11 R.F. Feldman and V.S. Ramachandran, Cem. Concr. Res., 4 (1974) 155.
12 V.S. Ramachandran and J.J. Beaudoin, J. Mater. Sci., 11 (1976) 893.
13 L. Ben-Dor, D. Perez and S. Sarig, J. Am. Ceram. Soc., 58 (1975) 87.
14 L. Ben-Dor and D. Perez, Thermochim. Acta, 12 (1975) 81.
15 L. Ben-Dor and D. Perez, Spectrochim. Acta, 18 (1979) 81.
16 L. Ben-Dor and Rubinsztain, Thermochim. Acta, 30 (1979) 9.
17 J. Bensted and S.P. Varma, Cem. Technol., 5 (1974) 440.
18 J. Bensted, Cem. Concr. Res., 9 (1979) 97.
19 J. Bensted, Torrind-Ztd, 102 (1978) 544.
20 J. Bensted, Cemento, 76 (1979) 117.
21 J. Bensted, Cemento, 88 (1980) 169.
22 N.B. Singh, Cem. Concr. Res., 5 (1975) 545.
23 N.B. Singh, Indian J. Technol., 15 (1977) 256.
24 D. Dollimore, G.A. Gamlen and R.J. Mangabhai, in D. Dollimore (Ed.), Proc. 2nd Eur. Symp. Therm. Anal., Heyden, London, 1981, p. 485.
25 H. Olmez, D. Dollimore, G.A. Gamlen and R.T. Mangabhai, SP79 American Concr. Inst. Detroit, 1 (1983) 607.
26 J.I. Bhatty, D. Dollimore, G.A. Gamlen, R.J. Mangabhai and H. Olmez, Thermochim. Acta, 106 (1986) 115.
27 J.I. Bhatty and K.J. Reid, Thermochim. Acta, 91 (1985) 95.
28 J.I. Bhatty, Thermochim. Acta, 106 (1986) 93.
29 J.I. Bhatty, Thermochim. Acta, 119 (1987) 235.
30 J.I. Bhatty, K.J. Reid, D. Dollimore, G.A. Gamlen, R.J. Mangabhai, P.F. Rogers and T.H. Shah, in C.M. Earnest (Ed.), Compositional Analysis by Thermogravimetry, ASTM STP 997, ASTM, Philadelphia, 1988, p. 204.
31 D. Dollimore, G.A. Gamlen, G.R. Heal and P.F. Rodgers, in D. Dollimore (Ed.), Proc. 2nd Eur. Symp. Therm. Anal., Heyden, London, 1981, p. 489.
32 T. Mitsuda, Cem. Concr. Res., 3 (1973) 71.
33 J.A. Gard and H.F.W. Taylor, Cem. Concr. Res., 6 (1976) 667.
34 G.L. Kalousek, T. Mitsuda and H.F.W. Taylor, Cem. Concr. Res., 7 (1977) 305.

35 L.S. Dent-Glasser, Mohan K. Lachowski and H.F.W. Taylor, Cem. Concr. Res., 8 (1978) 733.
36 J. Skalny and I. Odler, Mag. Concr. Res., 19 (1967) 203.
37 J.N. Maycock and J. Skalny, Thermochim. Acta, 8 (1974) 167.
38 I. Jawed, W.A. Klemm and J. Skalny, J. Am. Ceram. Soc., 62 (1979) 461.
39 J.N. Kalyoncu, M.E. Tadros, A.M. Baratta and J. Skalny, J. Therm. Anal., 9 (1976) 233.
40 B. El-Jazairi, in D. Dollimore (Ed.), 1st. Eur. Symp. Therm. Anal., Heyden, London, 1976, p. 378.
41 B. El-Jazairi, Thermochim. Acta, 21 (1977) 381.
42 B. El-Jazairi and J.M. Illston, Cem. Concr. Res., 7 (1977) 247.
43 B. El-Jazairi and J.M. Illston, Cem. Concr. Res., 10 (1980) 361.
44 H.G. Midgley and B. Rosaman, 4th ISCC, Washington, 1 (1962) 259.
45 H.G. Midgley, Cem. Concr. Res., 9 (1979) 77.
46 M.R. Rixom and N.P. Mailvaganam, Chemical Admixtures for Concrete, 2nd edn., E and F.N. Spon Ltd., London, 1986, p. 4.
47 V.S. Ramachandran (Ed.), Concrete Admixture Handbook—Properties, Science and Technology, Noyes Publications, New Jersey, 1984.
48 C.R. Wilding, A. Walter and A.A. Double, Cem. Concr. Res., 14(2) (1984) 185.
49 H.G. Midgely, Proc. 4th Int. Symp. Chem. Cem., Washington, 1960, p. 479.
50 F. Tamas, Proc. 6th Conf. Silicate Ind., Budapest, 1961, p. 425.
51 A. Petzold and I. Gohlert, Tonind.-Ztg. Keram. Rundsch., 86 (1962) 228.
52 R.Sh. Mikhail, A.T. Hussain and V.K. Gouda, Mag. Concr. Res., 19 (1967) 143.
53 D. Dollimore, G.A. Gamlen, R.J. Mangabhai and H. Olmez, in M.M. Chowdhury (Ed.), Proc. 14th NATAS Conf., San Francisco, 1985, p. 360.
54 V. Satava and O. Veprek, Zem. Kalk. Gips., 28 (1975) 170.
55 V. Satava and O. Veprek, Zem. Kalk. Gips., 28 (1975) 424.
56 V. Satava and O. Veprek, J. Am. Ceram. Soc., 58 (1975) 537.
57 V.M. Chebotnikov and A.B. Shalinets, Chem. Abstr., 86 (1977) 59552.
58 V. Lorprayon and D.R. Rossington, Can. Concr. Res., 11 (1981) 267.
59 R.F. Feldman and V.S. Ramachandran, Mag. Concr. Res., 18 (1966) 185.
60 R.F. Feldman and V.S. Ramachandran, J. Am. Ceram. Soc., 49 (1966) 268.
61 M. Collepardi, S. Monosi, G. Moriconi and M. Corradi, Cem. Concr. Res., 9 (1979) 431.
62 M. Collepardi, S. Monosi, G. Moriconi and M. Corradi, Cem. Concr. Res., 10 (1980) 455.
63 M. Collepardi, G. Baldini and M. Pauri, J. Am. Ceram. Soc., 62 (19) 33.
64 G.L. Kalousek and M. Adam, Proc. Am. Concr. Inst., 48 (1952) 77.
65 V.S. Ramachandran, Thermochim. Acta, 3 (1972) 343.
66 V.S. Ramachandran, in B. Miller (Ed.), Thermal Analysis–Proc. 7th Int. Conf. Therm. Anal., Vol. 2, Wiley, Chichester, U.K., 1982, p. 1296.
67 N.B. Singh and P.N. Ojha, J. Mater. Sci., 16 (1981) 2675.
68 V.S. Ramachandran, Mater. Constr. (Paris), 4 (1971) 3.
69 W. Richartz, Zem. Kalk. Gips., 10 (1967) 447.
70 H.G. Midgley and J.M. Illston, Cem. Concr. Res., 14(4) (1984) 546.
71 M. Kawamura, O.A. Kayyali and M.N. Haque, Cem. Concr. Res., 18(5) (1988) 763.
72 K. Suzuki, T. Nishikawa, H. Ikeaga and S. Ito, Cem. Concr. Res., 16(3) (1986) 333.
73 N.P. Stukalova and E.P. Andreeva, Kolloidn Zh., 31 (1969) 446.
74 N.B. Singh and K.M. Abha, Cem. Concr. Res., 13(5) (1983) 619.
75 J. Bensted, Cements, 75(1) (1978) 13.
76 K. Murakami and H. Tanaka, 5th Int. Symp. Chem. Cem., Vol. 2, Tokyo, 1968, p. 422.
77 V.S. Ramachandran, Thermochim. Acta, 127 (1988) 385.
78 P.P. Pudnikov, V.M. Kolbasov and A.S. Penteleev, Tsement, 27 (1968) 5.
79 J.F. Young, Mag. Concr. Res., 14 (1962) 137.

80 V.S. Ramachandran, Zem. Kalk. Gips., 31(4) (1978) 206.

81 N. Tenoutasse and N.B. Singh, Indian J. Technol., 16(5) (1978) 184.

82 V.S. Ramachandran and R.F. Feldman, Mater. Constr. (Paris), 5 (1972) 67.

83 M.R. Rixom and N.P. Mailvaganam, Chemical Admixtures for Concrete, 2nd Ed., E and F.N. Spon Ltd., London, 1986, p. 50.

84 V.S. Ramachandran, R.F. Feldman and J.J. Beaudoin, Concrete Science, Treatise on Current Research, Heyden, London, 1981.

85 M. Collepardi and M. Pauri, International Seminar on Calcium Aluminates, Turin, Italy, 1982.

86 M. Pauri, G. Ferrari and M. Collipardi, M. Cem. Concr. Res., 12 (1982) 271.

87 F. Massazza, U. Costa and A. Barrila, J. Am. Ceram. Soc., 65 (1982) 203.

88 V.S. Ramachandran and R.F. Feldman, Cem. Technol., 2(4) (1971) 121.

89 F. Massazza and U. Costa, Proc. 7th Int. Symp. Chem. Cem., Paris, 4, 1980, p. 259.

90 J.F. Young, Proc. 5th Int. Symp. Chem. Cem., Tokyo, 2 (1968) 256.

91 N.B. Milestone, Cem. Concr. Res., 7 (1977) 45.

92 R. Sersale, V. Sabatelli and G.L. Valenti, Proc. 7th Int. Symp. Chem. Cem., Paris, 4 (1980) 546.

93 S. Monosi, G. Moriconi and M. Collepardi, Cem. Concr. Res., 12 (1982) 425.

94 N.B. Milestone, J. Am. Ceram. Soc., 62 (1979) 321.

95 J.F. Young, J. Am. Ceram. Soc., 52 (1969) 44.

96 V.S. Ramachandran, 7th Int. Symp. Chem. Cem., Paris, 4 (1980) 535.

97 M. Collepardi, S. Monosi and G. Morconi, ref. 92, in Concrete Admixture Handbook—Properties, Science and Technology, V.S. Ramachandran (Ed.), Noyes Publication, New Jersey, 1984.

98 B. Blank, D.R. Rossington and L.A. Weinland, J. Am. Ceram. Soc., 46 (1963) 395.

99 N.B. Singh (Smt.), S.P. Singh and A.K. Singh, Cem. Concr. Res., 16(4) (1986) 545.

100 J.P. Gupta and J.I.H. Smith, in D. Dollimore (Ed.), Proc. 2nd Eur. Symp. Therm. Anal., Heyden, London, 1981, p. 483.

101 G. Dezhen, D. Xiong and L. Zhang, J. Am. Concr. Inst., 79(5) (1982) 378.

102 G.M. Bruere, Nature, 212 (1966) 502.

103 N.B. Milestone, Cem. Concr. Res., 14(2) (1984) 207.

104 P.C. Kreijger, Proc. Int. Symp. Adm. Mort. Conc, Brussels, Belgium, 1967, p. 33.

105 V.B. Ratinov and T.I. Rozenberg, in V.S. Ramachandran (Ed.), Concrete Admixture Handbook, Properties, Science and Technology, Noyes Publications, New Jersey, USA, 1984, p. 430.

106 V.B. Ratinov and T.I. Rozenberg, Additives in Concrete, Stroyizdat, Moscow, 1973, p. 207.